Research Paper

ROS-mediated lysosomal membrane permeabilization is involved in bupivacaine-induced death of rabbit intervertebral disc cells

Xianyi Cai[a,1], Yunlu Liu[a,1], Yiqiang Hu[a], Xianzhe Liu[a], Hongyan Jiang[b], Shuhua Yang[a], Zengwu Shao[a], Yun Xia[c,*], Liming Xiong[a,**]

[a] Department of Orthopaedics, Union Hospital, Tongji Medical College, Huazhong University of Science and Technology, Wuhan 430022, China
[b] Department of Otorhinolaryngology, Union Hospital, Tongji Medical College, Huazhong University of Science and Technology, Wuhan 430022, China
[c] Cancer Center, Union Hospital, Tongji Medical College, Huazhong University of Science and Technology, Wuhan 430022, China

ARTICLE INFO

ABSTRACT

Bupivacaine is frequently administered for diagnosing and controlling spine-related pain in interventional spine procedures. However, the potential cytotoxic effects of bupivacaine on intervertebral disc (IVD) cells and the underlying molecular mechanisms have not yet been fully established. Here, we showed that bupivacaine decreased the viability of rabbit IVD cells in a dose- and time-dependent manner. Moreover, the short-term cytotoxicity of bupivacaine in IVD cells was primarily due to cell necrosis, as assessed by Annexin V-propidium iodide staining and live/dead cell staining. Necrosis was verified by observations of swollen organelles, plasma membrane rupture, and cellular lysis under transmission electronic microscopy. Interestingly, our data indicated that bupivacaine-induced primary necrosis might involve the necroptosis pathway. The key finding of this study was that bupivacaine was able to induce lysosomal membrane permeabilization (LMP) with the release of cathepsins into the cytosol, as evidenced by LysoTracker Red staining, acridine orange staining, and cathepsin D immunofluorescence staining. Consistently, inhibitors of lysosomal cathepsins, CA074-Me and pepstatin A, significantly reduced bupivacaine-induced cell death. Finally, we found that bupivacaine resulted in an increase in intracellular reactive oxygen species (ROS) and that inhibition of ROS by N-acetyl-ʟ-cysteine effectively blocked bupivacaine-induced LMP and cell death. In summary, the results of this *in vitro* study reveal a novel mechanism underlying bupivacaine-induced cell death involving ROS-mediated LMP. Our findings establish a basis for the further investigation of bupivacaine cytotoxicity in an *in vivo* system.

1. Introduction

Low back pain, which is associated with intervertebral disc (IVD) degeneration, is a major factor that affects quality of life [1]. In recent years, local anesthetics have been frequently used for interventional spinal procedures to diagnose and treat spinal pain [2–4]. Despite being widely used in orthopedics, local anesthetics have been shown to be detrimental to various types of cells, such as articular chondrocytes [5], synovial cells [6], tenocytes [7], tenofibroblasts [8], and mesenchymal stem cells [9]. Several studies have recently demonstrated that a commonly used local anesthetic, bupivacaine, has direct cytotoxic effects on IVD cells [10–13]. In our previous studies, we showed that local anesthetics induced a concentration- and time-dependent decrease in the viability of IVD cells [14,15]. More importantly, an *in vivo* study suggested that the intradiscal injection of bupivacaine caused chondrotoxic effects in IVD cells [16]. However, the underlying mechanisms by which bupivacaine induces cytotoxicity remain largely unknown.

Lysosomes are cytoplasmic membrane-bound organelles that fill numerous hydrolytic enzymes capable of breaking down macromolecules and cell components [17]. Lysosomes have been long regarded as simple waste bags, although they are now known to play a crucial role in cell death [18,19]. Recent findings have suggested that the involvement of lysosomes in cell death is closely associated with lysosomal membrane permeabilization (LMP) [20,21]. It has been established that cell fate is dependent on the extent of lysosomal membrane damage; partial and selective lysosomal leakage results in apoptotic cell death, while massive rupture of lysosomes and rapid leak of lysosomal proteases into the cytosol lead to necrosis [20,22].

However, it is unknown whether lysosomes are implicated in bupivacaine-induced IVD cell death.

In the present study, we first investigated the short-term cytotoxic effect of bupivacaine on rabbit annulus fibrosus (AF) and nucleus pulposus (NP) cells *in vitro* and characterized the type of cell death induced by bupivacaine. In addition, we studied the molecular mechanisms of cytotoxicity by evaluating the role of reactive oxygen species (ROS) and the lysosomal pathway in the process of cell death.

2. Materials and methods

2.1. Isolation and culture of primary IVD cells

All experimental procedures were approved by the Animal Care and Ethics Committee of Huazhong University of Science and Technology. The isolation and culture of primary IVD cells (AF and NP) were performed according to our previous protocol [14,15]. Briefly, AF and NP cells were sampled from the thoracolumbar spine (L5-T10) of 3-month-old Japanese white rabbits and plated in Dulbecco's modified Eagle's medium/Ham's F-12 (DMEM/F-12; Gibco, Grand Island, NY, USA) with appropriate concentrations of fetal bovine serum (10%, 20%, respectively) (Gibco, USA) at 37 ℃ in a humidified atmosphere of 5% CO_2. The cells were then expanded until the second passage. Second-generation IVD cells were seeded at a density of 1.2×10^4 cells/well in 96-well plates, 2.5×10^5 cells/well in 6-well plates, or 5×10^4 cells/well in 24-well plates and used for subsequent experiments when they reached 80–90% confluence.

2.2. Treatment groups

To assess the dose-dependent effect of bupivacaine, AF and NP cells were exposed for 60 min to 0.125%, 0.25%, 0.375%, or 0.5% bupivacaine (Zhaohui Pharm, China) or 0.9% saline solution. To evaluate the time-dependent effect of bupivacaine, rabbit AF and NP cells were exposed to 0.9% saline solution or 0.375% bupivacaine for 0, 30, 60, 90, and 120 min. Normal (0.9%) saline solution served as a control because it was the primary component of the bupivacaine solutions used here. The 0.5% bupivacaine solution was used as provided by the manufacturer, and the lower-concentration bupivacaine solutions were diluted from 0.5% bupivacaine with 0.9% saline solution.

2.3. Cell counting kit-8 assay

The cytotoxic effect of bupivacaine on AF and NP cells was assessed using a CCK-8 colorimetric assay (Dojindo, Japan) as described previously [14,15,23]. Briefly, cells were resuspended and seeded in 96-well plates. After incubation for 48 h, cells were exposed to bupivacaine as described above. Afterwards, the supernatants were removed and replaced with 100 μl of fresh medium containing 10 μl of CCK-8 solution. After incubation for 4 h at 37 ℃ in the dark, the absorbance was measured at 450 nm using a microplate reader (Biotek, Winooski, VT, USA).

2.4. Annexin V–propidium iodide staining

Cell death was measured by flow cytometry using Annexin V and propidium iodide (PI) (KeyGen Biotech, China) staining as described previously [14,15,23]. Briefly, after treating with the designated concentrations of bupivacaine, cells were harvested and resuspended in 500 μl of Annexin V-FITC binding buffer, and then 5 μl of Annexin V and 5 μl of PI were added to each specimen according to the manufacturer's instructions. Samples were analyzed by flow cytometry (Becton Dickinson, Franklin Lakes, NJ, USA) using CellQuest analysis software (BD, USA).

2.5. Live/dead cell staining

Live and dead cells were detected using calcein acetoxymethyl ester (calcein AM) and PI (Sigma-Aldrich, St. Louis, MO, USA), respectively. Briefly, cells were seeded into 6-well plates and incubated for 48 h. After the corresponding treatment, the supernatants were discarded, and the wells were washed gently once with phosphate-buffered saline (PBS). Calcein AM (2 μM) and PI (1.5 μM) were added to each well to stain cells for 15 min at 37 ℃ in the dark. After staining, the cells were washed with PBS and imaged by fluorescence microscopy (IX71, Olympus, Japan). Calcein AM fluoresced green in live cells, whereas PI fluoresced red in dead cells.

2.6. Transmission electron microscopy

The ultrastructure of IVD cells after exposure to bupivacaine was examined by transmission electron microscopy (TEM). Briefly, cells were collected after the indicated treatments, washed twice with PBS, and pelleted by centrifugation at $300 \times g$ for 15 min. The pellets were fixed with 2.5% glutaraldehyde in PBS for 2 h at room temperature and post-fixed with 1% osmium tetroxide for 2 h at room temperature. After dehydration in a graded series of ethanol, the cells were embedded in Epon-812. Ultrathin sections were contrasted with uranyl acetate and lead citrate and were observed by using a Tecnai G2 12 transmission electron microscope (FEI Company, Holland).

2.7. Western blot analysis

After the indicated treatments, the total protein of IVD cells was extracted using a Western and IP cell lysis kit (Beyotime, China). The protein concentrations were measured using a BCA protein assay kit (Beyotime, China). Equal protein amounts (30 μg) were resolved on 10–12% SDS-PAGE gel and then transferred onto PVDF membranes (Millipore, Burlington, MA, USA). After blocking with 5% nonfat milk in TBST for 2 h at room temperature, the membrane was washed with TBST and incubated overnight at 4 ℃ with primary antibodies. The following antibodies were used: anti-receptor-interacting protein kinase 1 (RIPK1; 1:1000, Beverly, MA, CST, USA), anti-RIPK3 (1:1000, Abcam, Cambridge, MA, USA), anti-mixed lineage kinase domain-like (MLKL; 1:1000, Abcam, USA), and anti-GAPDH (1:1000, MultiSciences Biotech, China). Subsequently, the membranes were washed with TBST and incubated with the appropriate horseradish peroxidase-conjugated secondary antibodies for 60 min at room temperature. Protein bands were visualized using an enhanced chemiluminescence kit (Thermo, Rockford, IL, USA) as described previously [15]

2.8. Lysosomal staining

Lysosomal staining was performed using the lysosomotropic probe LysoTracker Red DND-99 (LTR; Invitrogen, Carlsbad, CA, USA). Briefly, cells were collected after exposure to bupivacaine, washed once with PBS, and resuspended in 1 ml fresh prewarmed medium containing 100 nM LTR. The cells were then maintained in the dark for 90 min at 37 ℃. The cells were washed with DMEM/F-12 twice after incubation, and the mean fluorescence intensity (MFI) was determined by flow cytometry (BD LSR II, Becton Dickinson) using FlowJo V 7.6.1 software (Tree Star, Olten, Switzerland). Stained lysosomes *in situ* were also visualized by laser-scanning confocal microscopy (Nikon A1, Japan).

2.9. Lysosomal membrane stability

Acridine orange (AO; Sigma-Aldrich, USA) was used to assess lysosomal membrane stability by two complementary experiments as described previously [24,25]. AO, a lysosomotropic weak base, accumulates in acidic compartments on the basis of proton trapping. AO is also known as a metachromatic fluorescent dye, for which fluorescence

emission depends on its concentration. In intact lysosomes with high concentrations, AO emits red fluorescence; in the cytosol and the nucleus with low concentrations, it emits green fluorescence [20]. Therefore, lysosomal membrane stability can be determined by detecting changes in either green fluorescence (AO relocation) or red fluorescence (AO uptake).

For AO relocation experiments, IVD cells were first preincubated with AO solution (5 μg/ml) in complete medium for 15 min at 37 °C. The cells were then exposed to bupivacaine for 60 min, and the changes in green fluorescence were measured by flow cytometry analysis.

For AO uptake experiments, IVD cells were first treated with bupivacaine for 60 min and then stained with AO solution (5 μg/ml) in complete medium for 15 min. The changes in red fluorescence were determined by flow cytometry. The stained cells *in situ* were also visualized by laser-scanning confocal microscopy.

2.10. Immunofluorescence

After the indicated treatments, IVD cells were washed in PBS and fixed in 4% paraformaldehyde at room temperature for 15 min. The cells were then blocked for 30 min in 5% bovine serum albumin (BSA) diluted with 0.3% Triton X–100. The cells were incubated with anti-cathepsin D primary antibody (Abcam, USA) at a 1:50 dilution overnight at 4 °C in a dark humidified chamber. After washing, the cells were incubated with a fluorophore-conjugated secondary antibody for 60 min. Then, the cells were counterstained with DAPI in the dark for 5 min. Stained samples were visualized and photographed using laser-scanning confocal microscopy.

2.11. Measurement of cellular ROS levels

The intracellular ROS level was measured by 2′,7′-dichlorofluorescin diacetate (DCFH-DA; Sigma-Aldrich, USA) staining as described previously [15]. Briefly, the IVD cells were collected after the indicated treatments, washed once with PBS, and stained with 10 μM DCFH-DA in the dark at 37 °C for 20 min. After washing three times with DMEM/F-12, the IVD cells were analyzed by flow cytometry.

2.12. Statistical analysis

Cells extracted from one rabbit were used to perform each independent experiment; neither AF cells nor NP cells from different rabbits were mixed in any experiment. Data are expressed as the mean values ± standard deviation (SD) of three independent experiments. Data analysis was performed using SPSS 22.0. Differences between groups were determined by Student's t-test or one-way analysis of variance (ANOVA) with the Bonferroni post hoc test, where appropriate. A value of $P < 0.05$ was considered statistically significant.

3. Results

3.1. Bupivacaine decreases the viability of rabbit IVD cells in a dose- and time-dependent manner

To test the cytotoxic effects of bupivacaine on IVD cells, we used a CCK-8 assay to measure cell viability. The absorbance value of cells under untreated control conditions was set to 1. The cell viability of both AF and NP cells after exposure to 0.25%, 0.375%, and 0.5% bupivacaine was significantly reduced compared with that of the saline control (Fig. 1A). Both AF and NP cells exposed to bupivacaine also exhibited a time-dependent decrease in cell viability (Fig. 1B). Compared with the IVD cells treated with normal saline, those treated with 0.375% bupivacaine showed a significant reduction in viability at all time points ($P < 0.05$). These results demonstrate the dose- and time-dependent cytotoxic effects of bupivacaine on IVD cells.

3.2. Characterization of IVD cell death induced by bupivacaine

To identify the type of IVD cell death induced by bupivacaine, cell death was determined by Annexin V/PI staining and live/dead cell staining. After 60 min of exposure to bupivacaine, the increase in IVD cell death was predominantly due to cellular necrosis (PI-positive cells) (Fig. 2A). There was a significant increase in PI-positive cells with increasing concentration of bupivacaine, except 0.125% bupivacaine (Fig. 2B). Consistently, live/dead cell staining showed that the number of PI-positive cells (red fluorescence) increased in IVD cells after exposure to bupivacaine, while the number of live cells (green fluorescence) decreased (Fig. 2C). To further confirm that cell necrosis was induced by bupivacaine, we used TEM to observe morphological changes. After exposure to 0.5% bupivacaine, the IVD cells exhibited necrotic morphological features, as manifested by the swelling of organelles, disruption of the plasma membrane, and subsequent cellular lysis (Fig. 3). These multiple lines of evidence indicate that a short-term exposure of bupivacaine can cause rapid cell death, which is primarily related to necrosis, in cultured rabbit IVD cells.

3.3. Cytotoxicity of bupivacaine involves the necroptosis pathway

One form of regulated necrosis, which is referred to as necroptosis, has recently been found to contribute to several pathologies [26]. To investigate whether bupivacaine-induced cell death is related to necroptosis, Western blotting was performed to determine the expression of key proteins of the necroptosis pathway, such as RIPK1, RIPK3, and MLKL. As shown in Fig. 4A and B, the expression levels of RIPK1, RIPK3, and MLKL protein were increased in response to bupivacaine treatment. To further confirm the involvement of the necroptosis pathway in bupivacaine-induced cell death, IVD cells were pretreated with or without RIPK1 inhibitor necrostatin-1 (Nec-1, 20 μM), RIPK3 inhibitor GSK872 (4 μM), or MLKL inhibitor necrosulfonamide (NSA, 4 μM) before bupivacaine treatment. The results of the CCK-8 assay showed that the viability of IVD cells was significantly improved by Nec-1, GSK872, and NSA (Fig. 4C). Collectively, these findings imply that bupivacaine-induced primary necrosis may involve RIPK1/RIPK3/MLKL-mediated necroptosis.

3.4. Bupivacaine induces LMP in IVD cells

Loss of lysosomal membrane integrity, as in the case of LMP, may lead to necrotic cell death. To further explore the mechanisms underlying bupivacaine-induced cell death, we investigated its possible effects on lysosomes. For this purpose, we first monitored the changes in lysosomal compartments by LTR staining. The LysoTracker probe, a fluorescent acidotropic probe, is usually used to label and track acidic organelles (lysosomes) and can be detected by flow cytometry or fluorescence microscopy. Analysis of the cells by flow cytometry showed that the MFI of LTR staining was markedly increased in IVD cells after exposure to lower doses of bupivacaine (0.125% and 0.25%), although 0.125% bupivacaine only caused a detectable, but not significant, increase in MFI in AF cells. Interestingly, this increase was transient because it was not detectable at higher doses of bupivacaine (0.375% and 0.5%). Conversely, a significant decrease in MFI was observed in IVD cells exposed to higher doses of bupivacaine (0.375% and 0.5%) (Fig. 5A and B). To further confirm the lysosomal changes induced by bupivacaine, the stained lysosomes *in situ* were observed under confocal microscopy. In parallel, 0.125% and 0.25% bupivacaine treatment induced an increase in punctuated red fluorescence of cells, indicating an increased size of lysosomes, compared with saline control treatment. However, the red fluorescence spots were dramatically decreased in IVD cells following 0.375% and 0.5% bupivacaine treatment, indicating a disruption of lysosomes (Fig. 5C). These data imply that the lysosomes in IVD cells seem to first increase in size and then disintegrate with increasing bupivacaine concentrations.
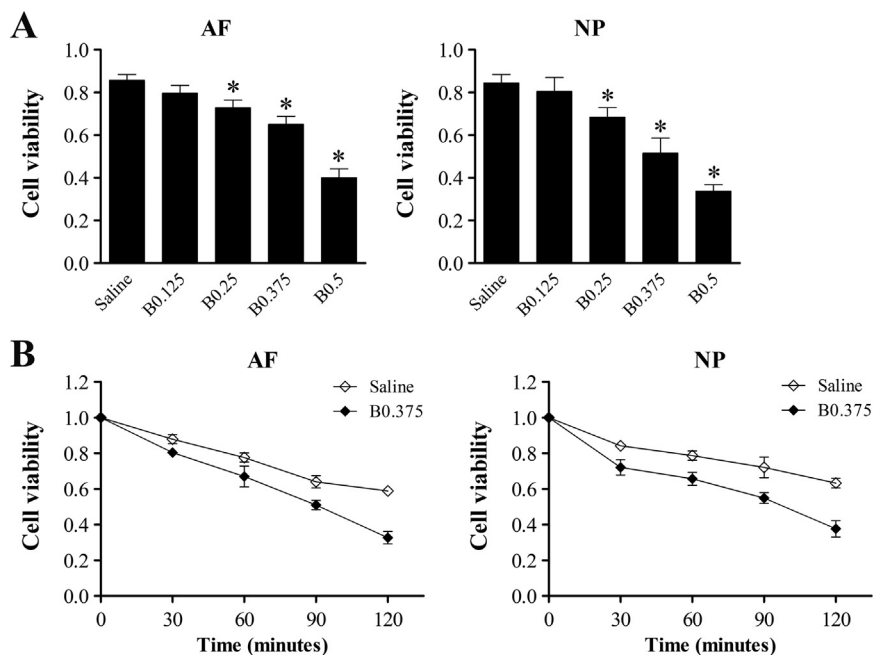
Fig. 1. Cytotoxic effects of bupivacaine on rabbit IVD cells. Cell viability was determined by CCK-8 assays. (A) CCK-8 assay dose-course. To determine the dose-dependent effects of bupivacaine, cells were treated with various concentrations of bupivacaine for 60 min or 0.9% saline as a control. (B) CCK-8 assay time-course. To illuminate the time-dependent effects of bupivacaine, cells were treated with 0.375% bupivacaine for 0, 30, 60, 90, and 120 min, and 0.9% saline was used as a control. The results are expressed as the means ± SD of three independent experiments ($^{*}P < 0.05$ vs saline control). AF, annulus fibrosus; NP, nucleus pulposus; B, bupivacaine.
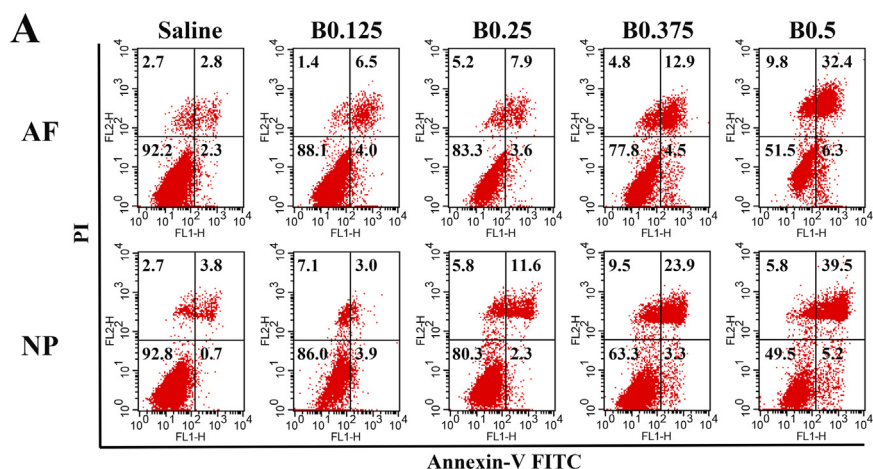

Fig. 2. Bupivacaine induces necrotic cell death in IVD cells. (A) Representative graphs obtained from flow cytometry analysis. After 60 min of exposure to bupivacaine, Annexin V/PI staining was performed to determine the type of cell death. Annexin-/PI- represents live cells, Annexin-/PI+ and Annexin + /PI+ represents necrotic cells, and Annexin + /PI- represents apoptotic cells. (B) Histogram analysis shows the percentage of PI-positive IVD cells. Data are presented as the means ± SD of three independent experiments ($^{*}P < 0.05$ vs. saline control). (C) Typical fluorescence photomicrograph of live/dead cell staining (Scale bars: 100 μm). Green fluorescence represents live cells, whereas red fluorescence represents necrotic cells. Photographs of green and red fluorescence were obtained under the same field and then merged. AF, annulus fibrosus; NP, nucleus pulposus; B, bupivacaine.
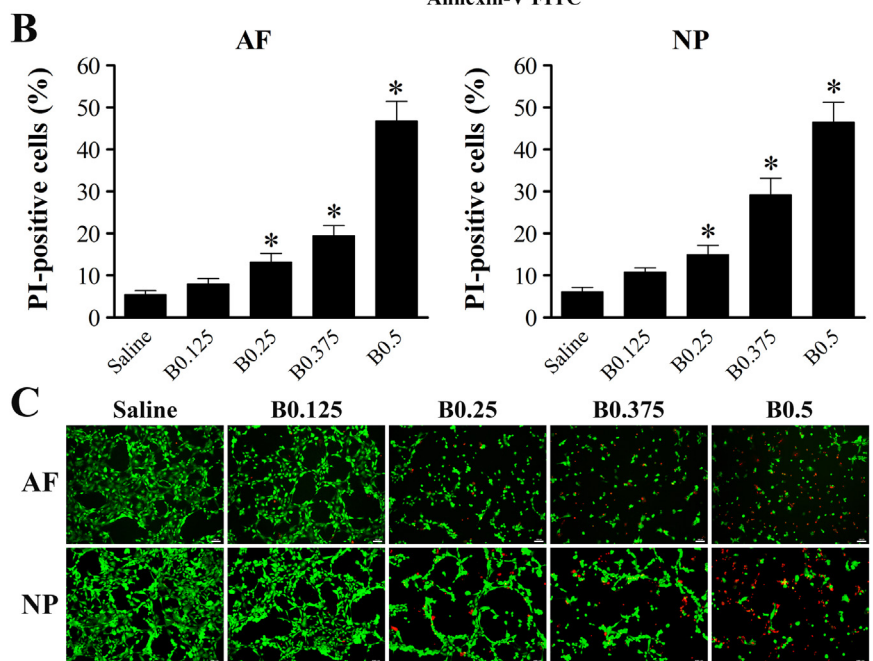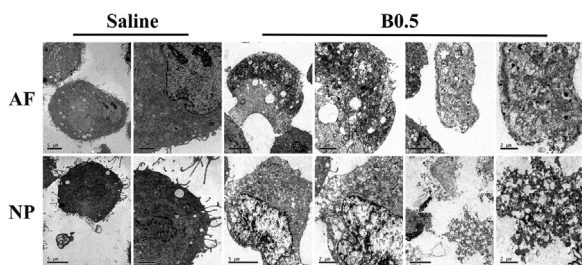
Fig. 3. Observations of the morphological ultrastructural appearance by TEM. The IVD cells exposed to saline displayed a nearly normal cell morphology, including plasma membrane integrity, abundant surrounding microvilli, and slight swelling of organelles. The IVD cells exposed to 0.5% bupivacaine showed typical necrotic morphological changes, including severe swelling of organelles, severe disruption of the plasma membrane, and cellular lysis. AF, annulus fibrosus; NP, nucleus pulposus; B, bupivacaine.

To investigate whether LMP actually occurred in IVD cells after bupivacaine treatment, two complementary experiments (AO relocation and AO uptake) were applied. Early alterations in lysosomal membrane stability can be detected in AO relocation experiments by evaluating the increase in green fluorescence [24,25]. After exposure to bupivacaine for 60 min, a dose-dependent increase in cellular green fluorescence was detected by flow cytometry, indicating the release of AO from ruptured lysosomes into the cytosol (Fig. 6A). Late lysosomal membrane damage can be detected in AO uptake experiments by

analyzing the decrease in red fluorescence. "Pale cells" were designed as cells with lower than normal red fluorescence [24,25]. The fraction of "pale cells" was markedly increased among both AF and NP cells after exposure to 0.375% or 0.5% bupivacaine, indicating late lysosomal membrane rupture, compared with exposure to saline control (Fig. 6B and C). To further confirm the effects of bupivacaine on lysosomal membrane rupture, cells after AO staining *in situ* were observed by confocal microscopy. As shown in Fig. 6D, the saline control cells showed bright lysosomal red and low cytosolic green fluorescence, indicating intact lysosomal membranes. However, there was a marked reduction in lysosomal red fluorescence accompanied by increased green cytosolic fluorescence when cells were exposed to bupivacaine, indicative of LMP. Altogether, these data demonstrate that bupivacaine can induce LMP in IVD cells.

3.5. Implication of lysosomal cathepsins in bupivacaine-induced death

Following lysosomal rupture, the translocation of cathepsins from the lysosomal lumen to the cytoplasm is an essential step leading to cell death. To determine the cytoplasmic relocation of cathepsins, we examined the subcellular distribution of cathepsin D in IVD cells after bupivacaine treatment by immunofluorescence techniques. Cathepsin D fluorescent staining was detected in a granular pattern representing intact lysosomes in saline-treated control cells. Exposure to bupivacaine caused a diffuse pattern, indicative of cathepsin D release from permeabilized lysosomes into the cytoplasm (Fig. 7A).
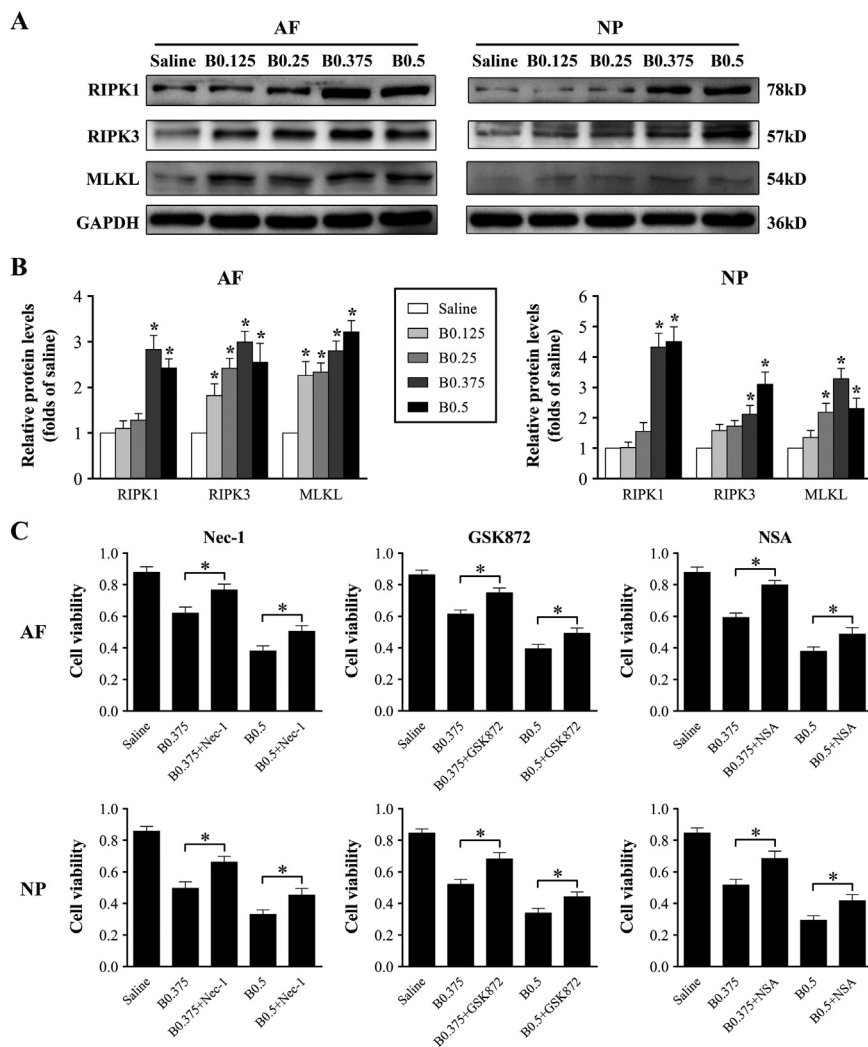

Fig. 4. Cytotoxicity of bupivacaine involves the necroptosis pathway. (A) Representative Western blots of the expression of RIPK1, RIPK3, and MLKL.

After exposure to bupivacaine for 60 min, the protein expression of RIPK1, RIPK3, and MLKL in IVD cells was determined by Western blot. (B) Histogram analysis showing the relative protein levels of RIPK1, RIPK3, and MLKL. Data are presented as the means ± SD of three independent experiments ($^*P < 0.05$ *vs.* saline control). (C) Protection of necroptosis inhibitors against bupivacaine-induced cytotoxicity. Before exposure to bupivacaine, IVD cells were preincubated with or without the RIPK1 inhibitor Nec-1 (20 μM), the RIPK3 inhibitor GSK872 (4 μM), or the MLKL inhibitor NSA (4 μM) for 60 min. After bupivacaine treatment, we assessed cell viability by CCK-8 assays. Data are presented as the means ± SD of three independent experiments ($^*P < 0.05$, Nec-1-treated, GSK872-treated, or NSA-treated *vs.* corresponding untreated cells). AF, annulus fibrosus; NP, nucleus pulposus; B, bupivacaine.
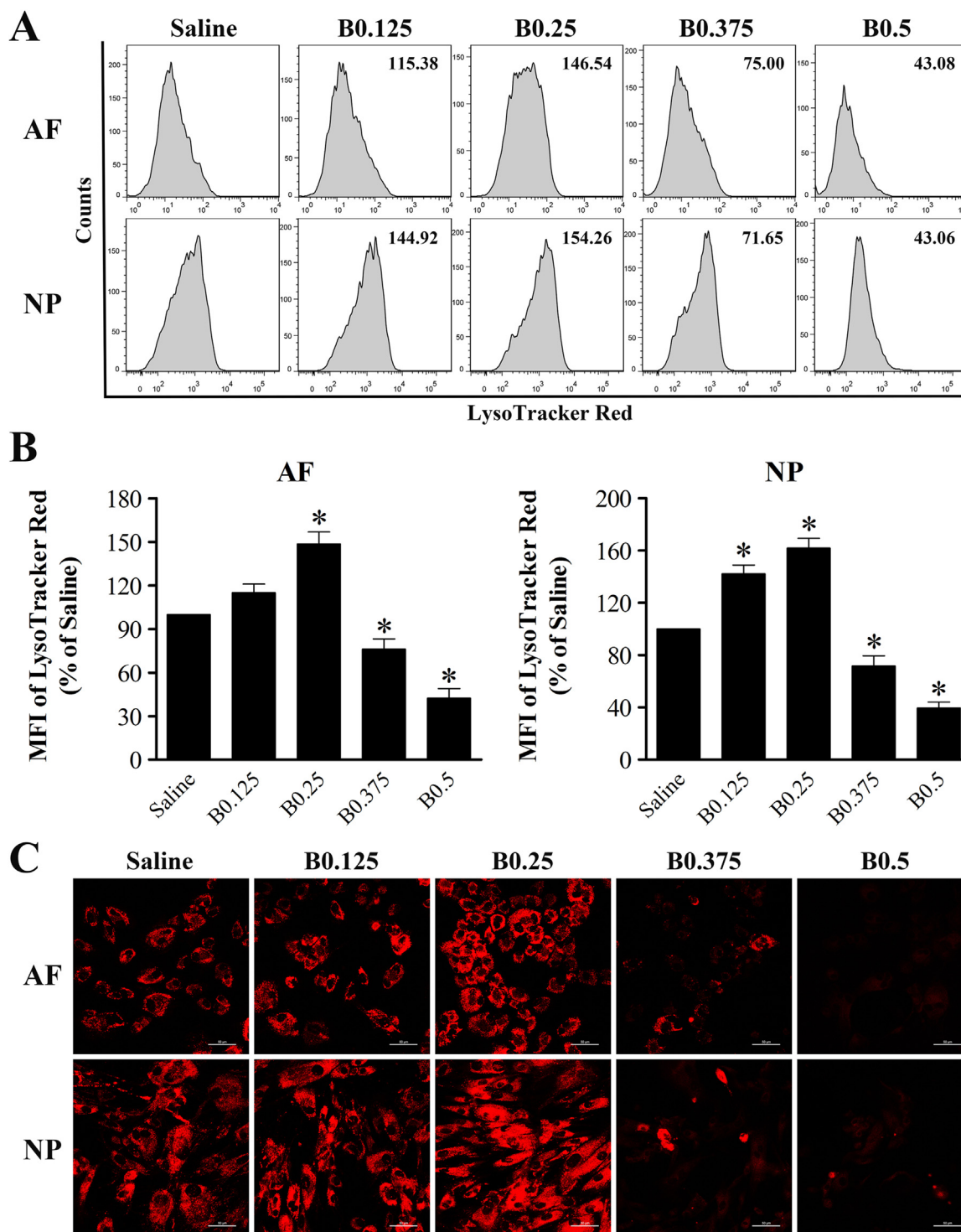
Fig. 5. Effect of bupivacaine on lysosomal compartments. After exposure to the indicated concentrations of bupivacaine, the lysosomal compartments in IVD cells was analyzed by LTR staining. (A) Representative graphs obtained from flow cytometry analysis. (B) Histogram analysis showing the MFI of LTR staining. Data are presented as the means ± SD of three independent experiments ($^*P < 0.05$ *vs.* saline control). (C) Typical confocal images of *in situ* LTR staining (Magnification ×400, scale bars = 50 μm). AF, annulus fibrosus; NP, nucleus pulposus; B, bupivacaine.

To investigate whether cysteine cathepsins participate in bupivacaine-induced cell death, IVD cells were pretreated with or without the cathepsin B inhibitor CA074-Me (20 μM) or the cathepsin D inhibitor pepstatin A (20 μM) before bupivacaine treatment. The cathepsin B inhibitor CA074-Me resulted in partial but significant protection against bupivacaine-induced cell death according to Annexin V/PI staining. Likewise, inhibition of cathepsin D by pepstatin A significantly

attenuated the cell death induced by bupivacaine (Fig. 7B and C). Taken together, these results supported the notion that bupivacaine-induced death of IVD cells is associated with LMP and the release of lysosomal cathepsins.
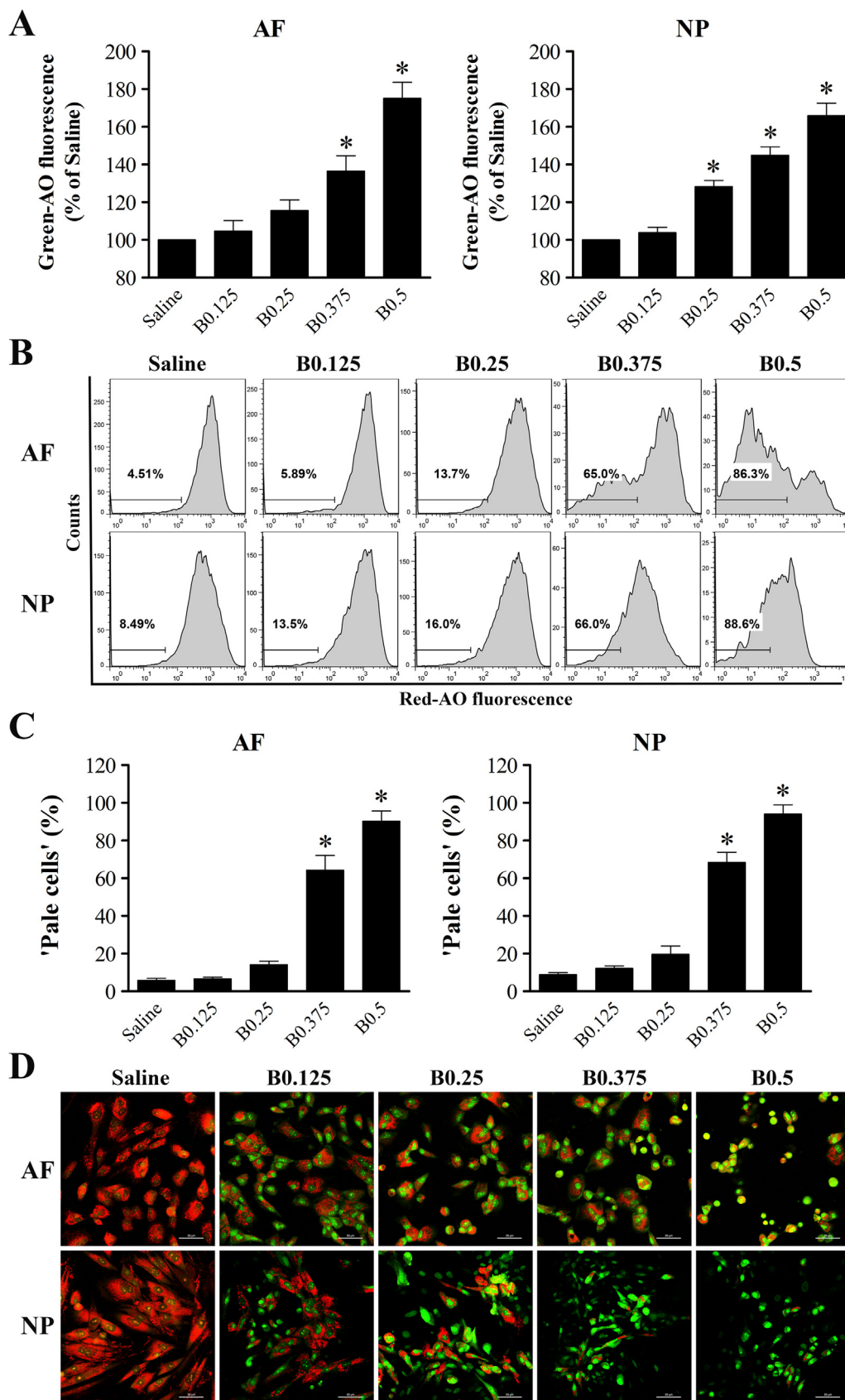
Fig. 6. Bupivacaine induces permeabilization of the lysosomal membrane. (A) Histogram representing the statistical analysis shows the MFI of green fluorescence in the AO relocation experiment. IVD cells were first preincubated with 5 μg/ml AO solution for 15 min with complete medium and then exposed to bupivacaine for 60 min. Green fluorescence was determined by flow cytometry. Data are presented as the means ± SD of three independent experiments ($^*P < 0.05$ vs. saline control). (B) Representative graphs of the AO uptake experiment obtained by flow cytometry analysis. IVD cells were first treated with bupivacaine for 60 min and then stained with 5 μg/ml AO solution in complete medium. Cells deficient in intact lysosomes ("pale cells") were determined by flow cytometry. (C) Histogram analysis showing the percentage of "pale cells". Data are presented as the means ± SD of three independent experiments ($^*P < 0.05$ vs. saline control). (D) Typical confocal images of in situ AO staining (Magnification ×400, scale bars = 50 μm). AF, annulus fibrosus; NP, nucleus pulposus; B, bupivacaine.
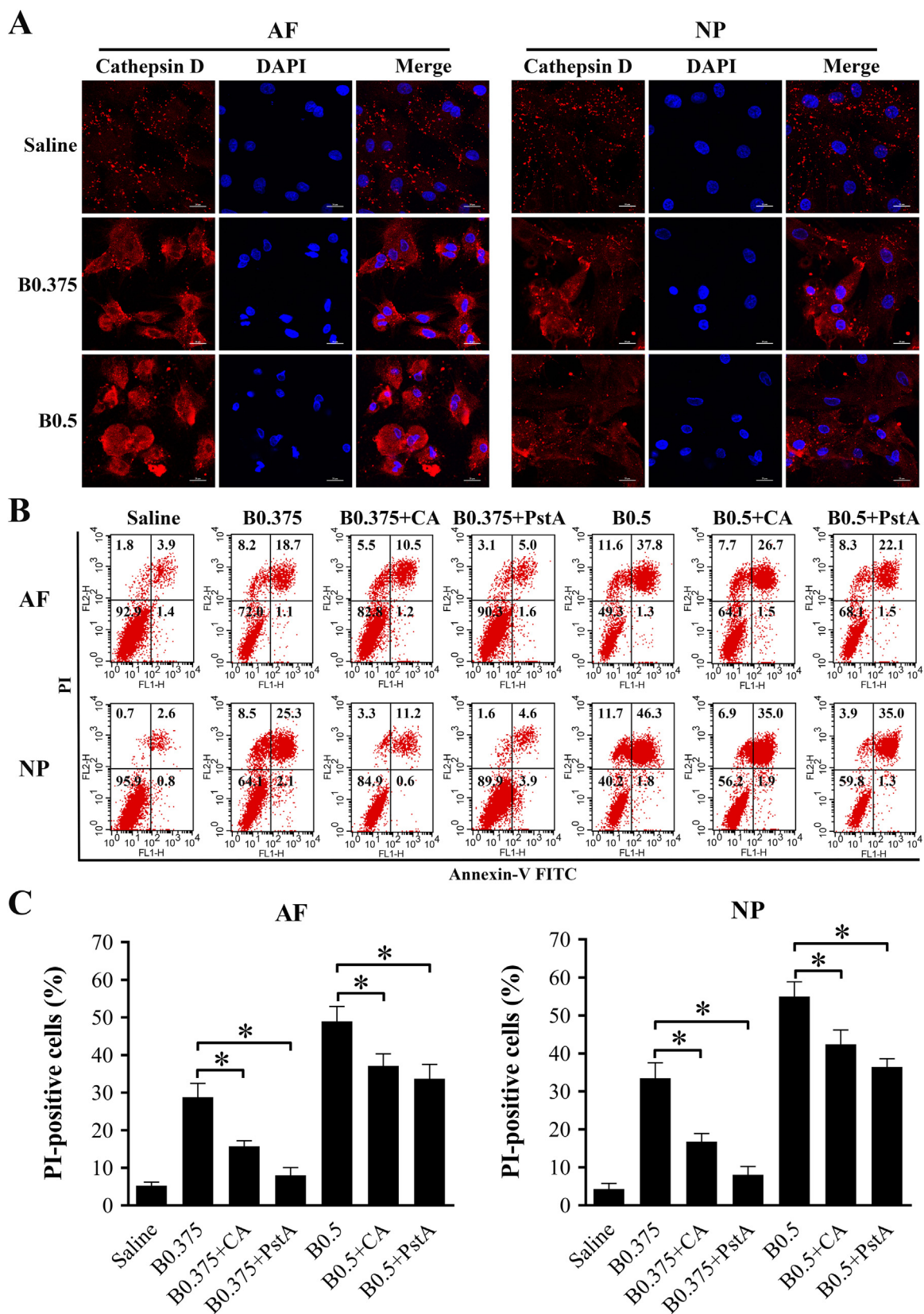
Fig. 7. Implication of lysosomal cathepsins in bupivacaine-induced cell death. (A) Typical confocal images of cathepsin D immunofluorescence staining in IVD cells after exposure to saline or bupivacaine (Magnification ×800, scale bars = 20 μm). (B) Representative graphs obtained from flow cytometry analysis after Annexin V/ PI staining. Before exposure to bupivacaine, the IVD cells were pretreated with or without the cathepsin B inhibitor CA074-Me (20 μM) or the cathepsin D inhibitor pepstatin A (20 μM) for 60 min. After bupivacaine treatment, cell death was assessed by flow cytometry. (C) Histogram analysis showing the percentage of PI-positive cells. Data are presented as the means ± SD of three independent experiments ($^*P < 0.05$, CA-treated or PstA-treated *vs.* corresponding untreated cells). AF, annulus fibrosus; NP, nucleus pulposus; B, bupivacaine; CA, CA074-Me; PstA, pepstatin A.
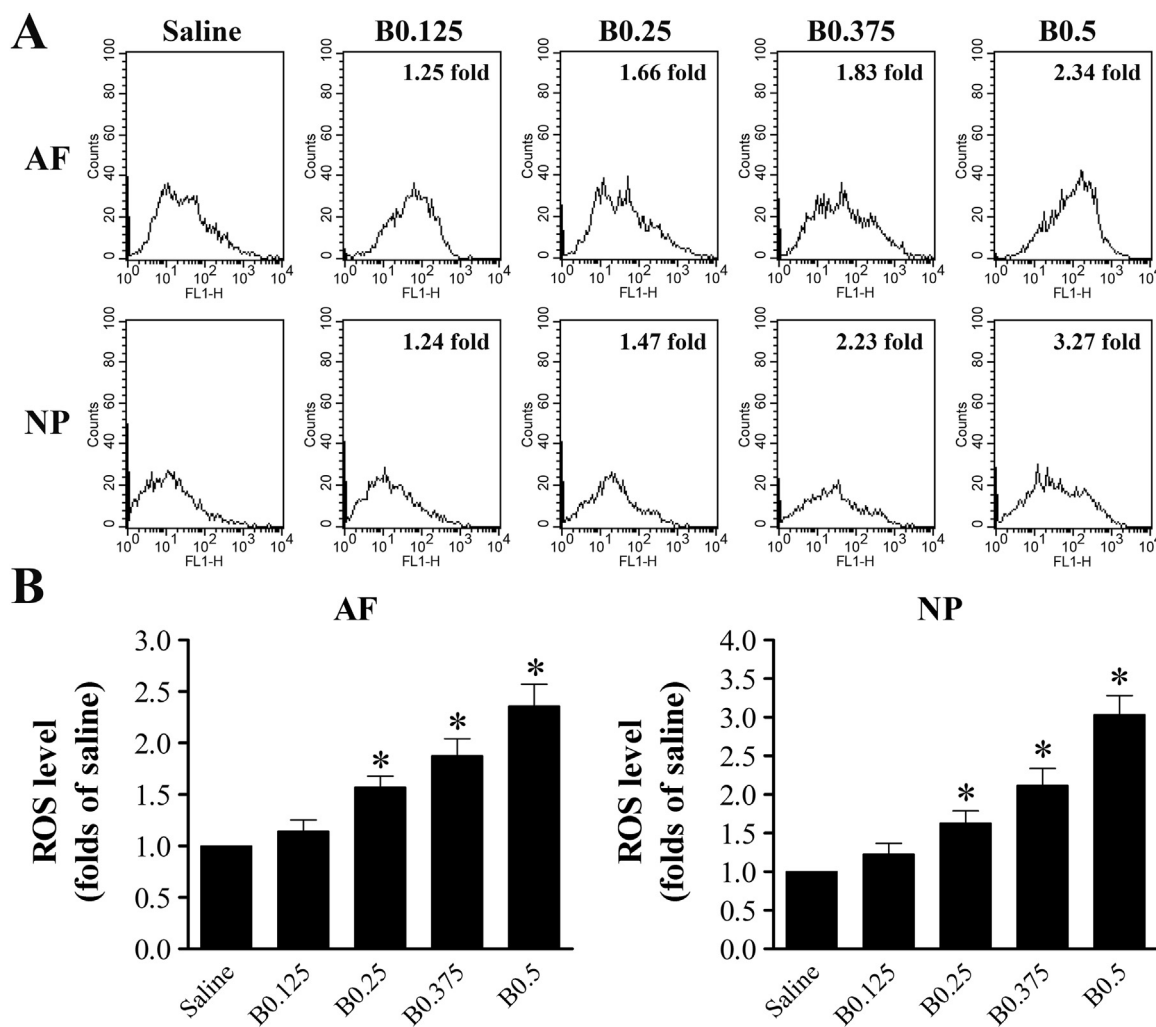
Fig. 8. ROS level increases in IVD cells after 60 min of treatment with bupivacaine. (A) Representative graphs obtained from flow cytometry analysis after fluorescent labeling with DCFH-DA. FL1-H: green. (B) Histogram analysis showing the intracellular ROS levels. Data are presented as the means ± SD of three independent experiments ($^*P < 0.05$ vs. saline control). AF, annulus fibrosus; NP, nucleus pulposus; B, bupivacaine.

3.6. ROS is an important mediator of bupivacaine-induced LMP and cell death

Oxidative stress caused by elevated cellular levels of ROS is one of the principal factors leading to LMP. To investigate whether ROS formation is involved in bupivacaine-triggered LMP and cell death, we first analyzed intracellular ROS levels by flow cytometry in response to bupivacaine treatment. As shown in Fig. 8, all concentrations of bupivacaine, except 0.125% bupivacaine, significantly increased ROS levels in both AF and NP cells in a dose-dependent manner. To examine whether bupivacaine-induced LMP and cell death could be prevented by inhibiting ROS generation, both AF and NP cells were pretreated with 5 mM N-acetyl-L-cysteine (NAC) for 60 min prior to bupivacaine treatment. Bupivacaine-induced ROS levels were markedly reduced by the antioxidant NAC (Fig. 9A and B). Notably, pretreatment with NAC significantly increased the MFI of LTR and reduced the proportion of "pale cells" (Fig. 9C–F). The addition of NAC significantly inhibited bupivacaine-induced death of IVD cells (Fig. 9G and H). Together, these results provide important evidence that ROS are involved in bupivacaine-induced LMP and cell death.

4. Discussion

Because of the widespread clinical use of bupivacaine in interventional spinal procedures, it is imperative to investigate the potential toxicity of bupivacaine on IVD cells and to explore the molecular mechanisms underlying bupivacaine-induced cell death. The present study shows that bupivacaine decreases the cellular viability of rabbit IVD cells in a dose- and time-dependent manner, which is consistent with the results of previous studies [10,14]. The novel finding of this study is that short-term exposure of rabbit IVD cells to bupivacaine causes increased induction of necrotic cell death, which involves RIPK1/RIPK3/MLKL-dependent necroptosis. More interestingly, our data provide the first evidence of the involvement of LMP in bupivacaine-induced death of IVD cells. Notably, ROS is a critical mediator in bupivacaine-induced LMP and cell death.

Cell death plays important roles in eliminating undesired, damaged, or infected cells during development, homeostasis, and pathogenesis. Historically, cell death has been subdivided into two major types: apoptosis and necrosis [27]. Apoptosis is characterized by cell shrinkage, DNA fragmentation, and activation of caspases [28]. In contrast to apoptosis, the key features of necrosis are organelle swelling, plasma membrane rupture, and cellular lysis [29]. The results of this study indicate that the characteristics of IVD cell death after short-term exposure to bupivacaine appear to be more related to necrotic cell death, as evidenced by a significant increase in PI-positive cells and the necrotic morphological changes observed by TEM. This finding is in agreement with previous reports by us and others suggesting that
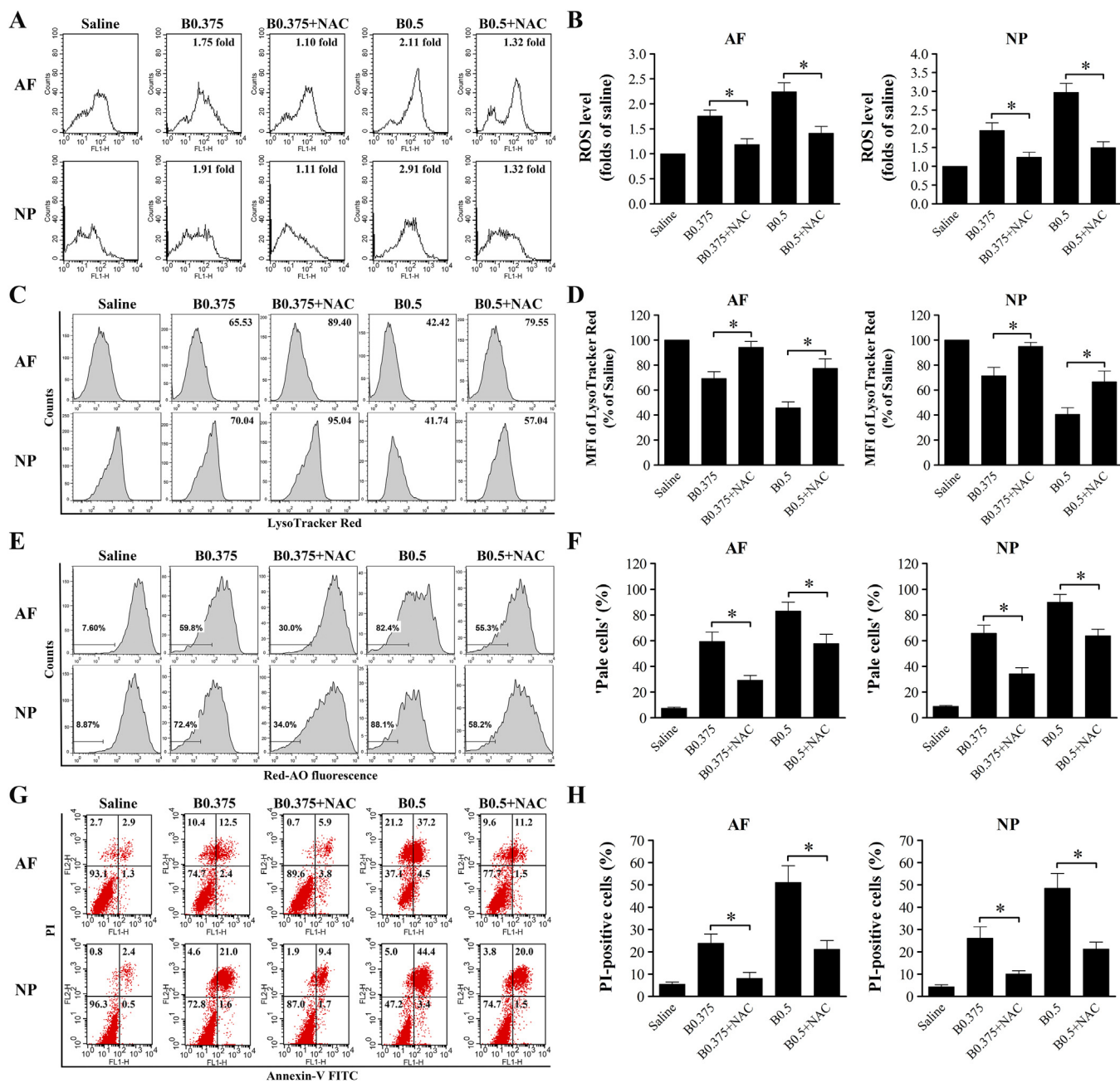
Fig. 9. ROS is an important mediator of bupivacaine-induced LMP and cell death. Prior to bupivacaine treatment, IVD cells were preincubated with or without 5 mM NAC for 60 min. (A, B) Effect of NAC on ROS production. (C, D) Effect of NAC on lysosomal compartments by LTR staining. (E, F) Effect of NAC on LMP by AO uptake experiments. (G, H) Effect of NAC on bupivacaine-induced cell death by Annexin V/PI staining. Data are presented as the means ± SD of three independent experiments (*$P < 0.05$, NAC-treated vs corresponding untreated cells). AF, annulus fibrosus; NP, nucleus pulposus; B, bupivacaine.

necrosis may be the main mechanism for the death of IVD cells after short-term exposure to bupivacaine [10,14]. Traditionally, necrosis has long been described as an uncontrolled form of cell death, but an increasing number of studies have shown that a regulated form of necrosis, termed necroptosis, is carried out by complex signal transduction pathways and execution mechanisms [29]. Necroptosis generally manifests with morphological features of necrosis and critically depends on RIPK1, RIPK3, and MLKL [30]. Our data showed that the protein levels of three key mediators of necroptosis, RIPK1, RIPK3, and MLKL, were markedly increased after exposure to bupivacaine. Accordingly, pretreatment with the RIPK1-specific inhibitor Nec-1, the RIPK3 inhibitor GSK872, or the MLKL inhibitor NSA significantly attenuated bupivacaine-induced cytotoxicity in IVD cells. Collectively, these results suggest that cell necrosis is the predominant form of IVD

cell death after short-term exposure to bupivacaine and that bupivacaine-induced primary necrosis may involve RIPK1/RIPK3/MLKL-dependent necroptosis.

The exact mechanisms involved in bupivacaine-induced death of IVD cells remain unclear. Previous studies have shown that bupivacaine affects mitochondrial function in other types of cells, such as chondrocytes [31–34]. Our previous results also suggested that mitochondria are one of the targets of bupivacaine related to its cytotoxicity on AF cells [15]. In addition to mitochondria, lysosomes have recently been shown to play a critical role in the progression of cell death [18,19]. Lysosomal cell death is initiated by LMP, which results in the release of cathepsins from the lysosomal lumen into the cytoplasm. Lysosomal cathepsin proteases ectopically present in the cytosol participate in the execution of subsequent cell death [35]. The results of
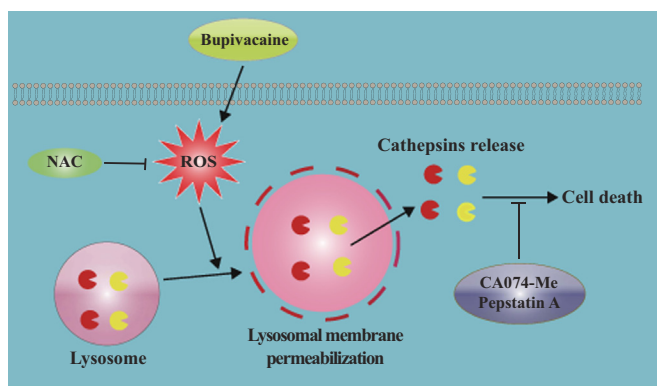
Fig. 10. Schematic illustration showing that ROS-mediated LMP is involved in bupivacaine-induced death of IVD cells.

earlier reports in other cell types suggested that bupivacaine may affect the activity of cathepsins and phospholipid metabolism in lysosomes [36–38]. However, the role of the lysosomal pathway in the process of bupivacaine-induced cell death has not yet been documented. In the current study, the results of LTR staining indicated that the disintegration of lysosomes is preceded by an increase in lysosomal size in IVD cells. Interestingly, lysosomal size alterations have been reported to be correlated with lysosomal instability and increased susceptibility to non-apoptotic cell death pathways [39,40]. Our study is the first to show based on various experimental approaches that exposure of IVD cells to bupivacaine leads to LMP with the release of cathepsins, such as cathepsin D, into the cytosol. Furthermore, the death induced by bupivacaine was markedly but not completely blocked by pretreatment with inhibitors of lysosomal cathepsins, such as CA074-Me and pepstatin A. These results imply that the mechanisms of bupivacaine-induced cell death are associated with increased LMP and cathepsin release.

After establishing the key role of LMP in bupivacaine-induced cell death, it is necessary to explore the possible mechanism by which bupivacaine destabilizes lysosome membranes in IVD cells. LMP can be induced by a large panel of distinct agents and endogenous molecules, but ROS-mediated LMP is the most studied mechanism of LMP [20]. ROS can easily diffuse into lysosomes and interact with free intralysosomal iron to generate highly reactive hydroxyl radicals in a Fenton-type reaction. Such a hydroxyl radical is then able to induce LMP by causing lipid peroxidation of lysosomal membranes and damaging lysosomal membrane proteins [35,41,42]. Previous studies have demonstrated that elevated levels of ROS appear to be particularly important in bupivacaine-induced cytotoxicity [8,15,43,44]. Thus, it is of interest to further explore the role of ROS in bupivacaine-induced LMP and cell death. Accordingly, we observed that treatment with bupivacaine stimulated IVD cells to generate ROS in a dose-dependent manner. Moreover, blockade of ROS production by NAC treatment significantly inhibited the extent of LMP and cell death. These results strongly suggest that increased ROS levels are responsible for bupivacaine-induced lysosomal damage and cell death.

There are several limitations to our study. First, we used monolayer NP cells to examine the direct cytotoxic effect of bupivacaine. Although a three-dimensional culture environment can maintain the physiologic phenotype of NP cells, a previous study showed that the cell death levels were similar in NP cells grown on a monolayer and on three-dimensional alginate beads after bupivacaine treatment [10]. Second, because of limited access to healthy human IVD tissue, rabbit IVD cells were used to determine the cytotoxicity of bupivacaine in healthy cells. Third, our experiments were performed *in vitro*, and *in vitro* results may not directly reflect clinical settings. Thus, the next step is to assess the *in vivo* cytotoxicity of bupivacaine on IVD cells. Fourth, our results presented are largely descriptive with only one aspect of toxicity pathway

explored. However, multiple organelle-specific pathways may participate in the initiation of bupivacaine-induced cell death. Therefore, further studies are needed to systematically investigate the roles of the nuclear, plasma-membrane-triggered, mitochondrial, reticular, lysosomal, and cytoskeletal pathways in bupivacaine-induced death of IVD cells.

In summary, we report, to the best of our knowledge, the first direct evidence that ROS-mediated LMP is involved in bupivacaine-induced death of IVD cells. A schematic of the proposed bupivacaine-induced cell death mechanism is summarized in Fig. 10. Our findings establish a basis for the further investigation of bupivacaine cytotoxicity in an *in vivo* system. If the toxicity results obtained in this *in vitro* study can be corroborated *in vivo*, caution regarding diagnosing and treating spine-related pain with bupivacaine will be necessary.

Acknowledgments

Author roles

XYC, YX, and LMX designed the study. XYC, YLL, YQH, XZL, HYJ, and YX conducted the experiments. XYC, YLL, YQH, and XZL analyzed the data. SHY, ZWS, and LMX supervised the experiments. XYC, YX, and LMX drafted the manuscript. SHY, ZWS, YX, and LMX revised the manuscript. All authors approved the final version of the manuscript.

Disclosures

None of the authors declare any competing interests.

References

[1] G.B. Andersson, Epidemiological features of chronic low-back pain, Lancet 354 (9178) (1999) 581–585.
[2] Y. Zhou, S. Abdi, Diagnosis and minimally invasive treatment of lumbar discogenic pain–a review of the literature, Clin. J. Pain 22 (5) (2006) 468–481.
[3] S. Ohtori, T. Kinoshita, M. Yamashita, et al., Results of surgery for discogenic low back pain: a randomized study using discography versus discoblock for diagnosis, Spine 34 (13) (2009) 1345–1348 (Phila Pa 1976).
[4] J.B. Staal, R.A. de Bie, H.C. de Vet, J. Hildebrandt, P. Nelemans, Injection therapy for subacute and chronic low back pain: an updated Cochrane review, Spine 34 (1) (2009) 49–59 (Phila Pa 1976).
[5] C.R. Chu, N.J. Izzo, N.E. Papas, F.H. Fu, In vitro exposure to 0.5% bupivacaine is cytotoxic to bovine articular chondrocytes, Arthroscopy 22 (7) (2006) 693–699.
[6] A.J. Rao, T.R. Johnston, A.H. Harris, R.L. Smith, J.G. Costouros, Inhibition of chondrocyte and synovial cell death after exposure to commonly used anesthetics: chondrocyte apoptosis after anesthetics, Am. J. Sports Med. 42 (1) (2014) 50–58.
[7] S.L. Piper, D. Laron, G. Manzano, et al., A comparison of lidocaine, ropivacaine and dexamethasone toxicity on bovine tenocytes in culture, J. Bone Jt. Surg. Br. 94 (6) (2012) 856–862.
[8] C.M. Sung, Y.S. Hah, J.S. Kim, et al., Cytotoxic effects of ropivacaine, bupivacaine, and lidocaine on rotator cuff tenofibroblasts, Am. J. Sports Med. 42 (12) (2014) 2888–2896.
[9] R. Rahnama, M. Wang, A.C. Dang, H.T. Kim, A.C. Kuo, Cytotoxicity of local anesthetics on human mesenchymal stem cells, J. Bone Jt. Surg. Am. 95 (2) (2013) 132–137.
[10] H. Lee, G. Sowa, N. Vo, et al., Effect of bupivacaine on intervertebral disc cell viability, Spine J. 10 (2) (2010) 159–166.
[11] L. Quero, M. Klawitter, A.G. Nerlich, M. Leonardi, N. Boos, K. Wuertz, Bupivacaine–the deadly friend of intervertebral disc cells? Spine J. 11 (1) (2011) 46–53.
[12] D. Wang, N.V. Vo, G.A. Sowa, et al., Bupivacaine decreases cell viability and matrix protein synthesis in an intervertebral disc organ model system, Spine J. 11 (2) (2011) 139–146.
[13] A.V. Chee, J. Ren, B.A. Lenart, E.Y. Chen, Y. Zhang, H.S. An, Cytotoxicity of local anesthetics and nonionic contrast agents on bovine intervertebral disc cells cultured in a three-dimensional culture system, Spine J. 14 (3) (2014) 491–498.
[14] X.Y. Cai, L.M. Xiong, S.H. Yang, et al., Comparison of toxicity effects of ropivacaine, bupivacaine, and lidocaine on rabbit intervertebral disc cells in vitro, Spine J. 14 (3) (2014) 483–490.
[15] X.Y. Cai, Y. Xia, S.H. Yang, et al., Ropivacaine- and bupivacaine-induced death of

rabbit annulus fibrosus cells in vitro: involvement of the mitochondrial apoptotic pathway, Osteoarthr. Cartil. 23 (10) (2015) 1763–1775.

[16] P. Strube, B.M. Pfitzner, F. Streitparth, T. Hartwig, M. Putzier, In vivo effects of bupivacaine and gadobutrol on the intervertebral disc following discoblock and discography: a histological analysis, Eur. Radiol. 27 (1) (2017) 149–156.

[17] P. Saftig, J. Klumperman, Lysosome biogenesis and lysosomal membrane proteins: trafficking meets function, Nat. Rev. Mol. Cell Biol. 10 (9) (2009) 623–635.

[18] U. Repnik, V. Stoka, V. Turk, B. Turk, Lysosomes and lysosomal cathepsins in cell death, Biochim. Biophys. Acta 1824 (1) (2012) 22–33.

[19] H. Appelqvist, P. Waster, K. Kagedal, K. Ollinger, The lysosome: from waste bag to potential therapeutic target, J. Mol. Cell Biol. 5 (4) (2013) 214–226.

[20] P. Boya, G. Kroemer, Lysosomal membrane permeabilization in cell death, Oncogene 27 (50) (2008) 6434–6451.

[21] U. Repnik, M. Hafner Cesen, B. Turk, Lysosomal membrane permeabilization in cell death: concepts and challenges, Mitochondrion 19 Pt A (2014) 49–57.

[22] A.C. Johansson, H. Appelqvist, C. Nilsson, K. Kagedal, K. Roberg, K. Ollinger, Regulation of apoptosis-associated lysosomal membrane permeabilization, Apoptosis 15 (5) (2010) 527–540.

[23] X. Cai, Y. Liu, W. Yang, et al., Long noncoding RNA MALAT1 as a potential therapeutic target in osteosarcoma, J. Orthop. Res. 34 (6) (2016) 932–941.

[24] X.M. Yuan, W. Li, H. Dalen, et al., Lysosomal destabilization in p53-induced apoptosis, Proc. Natl. Acad. Sci. USA 99 (9) (2002) 6286–6291.

[25] C.O. Eno, G. Zhao, A. Venkatanarayan, B. Wang, E.R. Flores, C. Li, Noxa couples lysosomal membrane permeabilization and apoptosis during oxidative stress, Free Radic. Biol. Med. 65 (2013) 26–37.

[26] T. Vanden Berghe, A. Linkermann, S. Jouan-Lanhouet, H. Walczak, P. Vandenabeele, Regulated necrosis: the expanding network of non-apoptotic cell death pathways, Nat. Rev. Mol. Cell Biol. 15 (2) (2014) 135–147.

[27] A. Degterev, J. Yuan, Expansion and evolution of cell death programmes, Nat. Rev. Mol. Cell Biol. 9 (5) (2008) 378–390.

[28] G. Kroemer, L. Galluzzi, P. Vandenabeele, et al., Classification of cell death: recommendations of the Nomenclature Committee on Cell Death 2009, Cell Death Differ. 16 (1) (2009) 3–11.

[29] T. Vanden Berghe, N. Vanlangenakker, E. Parthoens, et al., Necroptosis, necrosis and secondary necrosis converge on similar cellular disintegration features, Cell Death Differ. 17 (6) (2010) 922–930.

[30] L. Galluzzi, I. Vitale, S.A. Aaronson, et al., Molecular mechanisms of cell death: recommendations of the Nomenclature Committee on Cell Death 2018, Cell Death Differ. 25 (3) (2018) 486–541.

[31] W. Irwin, E. Fontaine, L. Agnolucci, et al., Bupivacaine myotoxicity is mediated by mitochondria, J. Biol. Chem. 277 (14) (2002) 12221–12227.

[32] O. Cela, C. Piccoli, R. Scrima, et al., Bupivacaine uncouples the mitochondrial oxidative phosphorylation, inhibits respiratory chain complexes I and III and enhances ROS production: results of a study on cell cultures, Mitochondrion 10 (5) (2010) 487–496.

[33] V. Grishko, M. Xu, G. Wilson, A.Wt Pearsall, Apoptosis and mitochondrial dysfunction in human chondrocytes following exposure to lidocaine, bupivacaine, and ropivacaine, J. Bone Jt. Surg. Am. 92 (3) (2010) 609–618.

[34] Y. Xing, N. Zhang, W. Zhang, L.M. Ren, Bupivacaine indirectly potentiates glutamate-induced intracellular calcium signaling in rat hippocampal neurons by impairing mitochondrial function in cocultured astrocytes, Anesthesiology 128 (3) (2018) 539–554.

[35] S. Aits, M. Jaattela, Lysosomal cell death at a glance, J. Cell Sci. 126 (Pt 9) (2013) 1905–1912.

[36] S. Ishiura, I. Nonaka, H. Sugita, Biochemical aspects of bupivacaine-induced acute muscle degradation, J. Cell Sci. 83 (1986) 197–212.

[37] E. Lucchinetti, A.E. Awad, M. Rahman, et al., Antiproliferative effects of local anesthetics on mesenchymal stem cells: potential implications for tumor spreading and wound healing, Anesthesiology 116 (4) (2012) 841–856.

[38] R. Li, H. Ma, X. Zhang, et al., Impaired autophagosome clearance contributes to local anesthetic bupivacaine-induced myotoxicity in mouse myoblasts, Anesthesiology 122 (3) (2015) 595–605.

[39] K. Ono, S.O. Kim, J. Han, Susceptibility of lysosomes to rupture is a determinant for plasma membrane disruption in tumor necrosis factor alpha-induced cell death, Mol. Cell Biol. 23 (2) (2003) 665–676.

[40] L. Groth-Pedersen, M.S. Ostenfeld, M. Hoyer-Hansen, J. Nylandsted, M. Jaattela, Vincristine induces dramatic lysosomal changes and sensitizes cancer cells to lysosome-destabilizing siramesine, Cancer Res. 67 (5) (2007) 2217–2225.

[41] M.H. Cesen, K. Pegan, A. Spes, B. Turk, Lysosomal pathways to cell death and their therapeutic applications, Exp. Cell Res. 318 (11) (2012) 1245–1251.

[42] A. Serrano-Puebla, P. Boya, Lysosomal membrane permeabilization in cell death: new evidence and implications for health and disease, Ann. N. Y. Acad. Sci. 1371 (1) (2016) 30–44.

[43] O. Galbes, A. Bourret, K. Nouette-Gaulain, et al., N-acetylcysteine protects against bupivacaine-induced myotoxicity caused by oxidative and sarcoplasmic reticulum stress in human skeletal myotubes, Anesthesiology 113 (3) (2010) 560–569.

[44] C. Lehner, R. Gehwolf, C. Hirzinger, et al., Bupivacaine induces short-term alterations and impairment in rat tendons, Am. J. Sports Med. 41 (6) (2013) 1411–1418.